QUANTUM GASES

Quantum scale anomaly and spatial coherence in a 2D Fermi superfluid

Puneet A. Murthy[1]*†‡, Nicolò Defenu[2]*†, Luca Bayha[1], Marvin Holten[1], Philipp M. Preiss[1], Tilman Enss[2], Selim Jochim[1]

Quantum anomalies are violations of classical scaling symmetries caused by divergences that appear in the quantization of certain classical theories. Although they play a prominent role in the quantum field theoretical description of many-body systems, their influence on experimental observables is difficult to discern. In this study, we discovered a distinctive manifestation of a quantum anomaly in the momentum-space dynamics of a two-dimensional (2D) Fermi superfluid of ultracold atoms. The measured pair momentum distributions of the superfluid during a breathing mode cycle exhibit a scaling violation in the strongly interacting regime. We found that the power-law exponents that characterize long-range phase correlations in the system are modified by the quantum anomaly, emphasizing the influence of this effect on the critical properties of 2D superfluids.

Symmetries and their violations are fundamental concepts in physics. A prominent type is conformal symmetry, which gives rise to the peculiar effect of scale invariance, where the properties of a system are unchanged under a transformation of scale. For instance, a Hamiltonian $H(x)$ is said to be scale invariant when $H(\lambda x) = \lambda^{\alpha} H(x)$, where λ is a scaling factor and α is a real number. Scaling symmetries such as these can be violated by quantum fluctuations, which is a phenomenon known as a quantum anomaly. Such anomalous symmetry breaking is widely discussed in quantum field theory (*1*) and has fundamental implications in the contexts of high-energy physics and phase transitions. However, unambiguous experimental signatures of this effect, particularly in many-body systems, have so far been elusive. Here, we report the direct observation of a quantum anomaly in the dynamics of a two-dimensional Fermi superfluid.

Two-dimensional (2D) systems with contact interactions, $V(x) \propto \delta^2(x)$, are of particular interest in the context of scale-invariance violation because the δ^2 potential does not introduce a characteristic scale to the Hamiltonian. At the classical level, the transformation $x \rightarrow \lambda x$ rescales the interaction potential as $V(\lambda x) \propto \lambda^{-2} V(x)$, exactly the same way as the kinetic energy, and therefore the classical 2D gas is intrinsically scale invariant (*2*, *3*). However, at the quantum mechanical level, this is no longer true because the δ^2 scattering potential supports a two-body bound state for arbitrarily weak attraction (*4*–*6*). The bound state has a characteristic length a_{2D}, which describes the expected size of the molecule and introduces a spatial scale. This additional length scale is connected with the binding energy scale E_B, and it breaks the scaling relation between interaction and kinetic energy, which leads to a quantum anomaly.

How does this quantum anomaly influence the behavior of 2D systems at macroscopic scales? This question is especially relevant for 2D superfluids, which exhibit algebraic, hence scale-free, decay of phase correlations (*7*, *8*) described by the Berezinskii-Kosterlitz-Thouless (BKT) mechanism. In this context, how does the introduction of a short-distance scale (a_{2D}) affect the long-range behavior, such as spatial coherence and transport properties, in 2D superfluids? These questions are at the heart of many-body physics of 2D systems, and answering them may provide insights into the general phenomenology of other lower dimensional systems such as exciton-polariton condensates (*9*) and graphene (*10*, *11*).

In the field of ultracold atomic gases, 2D Bose gases in the weakly repulsive instead of interacting limit are demonstrably scale invariant (*3*, *12*, *13*), suggesting that the bound state plays a negligible role in these systems. However, in 2D Fermi gases, particularly in the strongly interacting regime, the effect of the additional length scale a_{2D} becomes appreciable, for instance in the thermodynamic equation of state (*14*–*19*). On this basis, various theoretical works have predicted a quantitatively pronounced effect of the scale-invariance violation in this regime (*20*–*23*).

In harmonically trapped gases, a notable manifestation of this anomaly is an interaction-induced correction to the collective breathing mode frequency with respect to the noninteracting value (*4*, *20*–*22*, *24*) of twice the trap frequency. Although previous studies on breathing modes found no evidence of such a correction (*25*), the observation of an anomalous frequency shift at low temperatures has been reported in recent experiments (*26*, *27*). However, the relative magnitude of these shifts (~1 to 2%) is several times smaller than the theoretical prediction (~10%), raising questions on the physical relevance of the quantum anomaly for the dynamical properties of 2D Fermi gases. Rather than the breathing mode frequencies, here we explore the spatial coherence properties in momentum space, which reveal the scale-invariance breaking effect that is nearly absent in the position-space density profiles.

In our experiments, we prepared a gas of ~2×10^4 ^{6}Li atoms in the lowest two hyperfine states, trapped in a highly anisotropic potential and cooled to low temperatures deep in the superfluid phase. The ratio of absolute temperature to the Fermi temperature (T/T_F) is in the range of ~0.05 to 0.1. The radial and axial trap frequencies of the harmonic potential are $\omega_r = 2\pi \times 23$ Hz and $\omega_z = 2\pi \times 7.1$ kHz, respectively, corresponding to an aspect ratio $\omega_z/\omega_r \approx 310$. With the relevant thermodynamic scales kept smaller than the axial confinement energy, we ensure that the system is in the kinematically 2D regime. By tuning the interactions between fermions around a Feshbach resonance, we access the 2D Bose-Einstein condensate to the Bardeen-Cooper-Schrieffer (BEC-BCS) crossover region. The interactions in the 2D many-body system are described by a dimensionless parameter $\ln(k_F a_{2D})$, where k_F is the Fermi momentum and a_{2D} is the 2D scattering length obtained from the 3D scattering length (*5*, *6*, *28*). For $\ln(k_F a_{2D}) \ll -1$, we are in the BEC regime, whereas $\ln(k_F a_{2D}) \gg 1$ corresponds to the BCS regime. The strongly correlated regime located between these limits occurs when $1/k_F \sim a_{2D}$. This crossover region exhibits some notable features, such as enhanced critical temperature T_c (*14*) and a large pseudogap region above T_c where pairing is strongly density dependent (*29*).

We investigated the interplay between quantum anomaly and phase correlations by measuring the dynamical evolution of the gas both in position space (i.e., in situ) and in momentum space. Measuring the momentum distribution is particularly important as it encodes information of phase fluctuations in the superfluid. First, we brought the system out of its equilibrium configuration by resonantly modulating the harmonic trapping potential at twice the trap frequency $2\omega_r$ (Fig. 1, A and B). This protocol excites the 2D isotropic breathing mode whereby the gas undergoes periodic cycles of compression and expansion. After a fixed duration (10 cycles), the drive was stopped, and the cloud evolved in the original potential for a variable time *t*. In contrast to previous works, which investigated the frequency of the breathing mode, we focus on how the shapes of the in situ and momentum distributions change within a single breathing cycle. Because the damping rate of the breathing mode is very small (~$0.01\omega_r$) (*26*), the motion is essentially isentropic, which allows the direct probing of scale-invariant behavior.

[1]Physics Institute, Heidelberg University, Heidelberg, Germany. [2]Institute for Theoretical Physics, Heidelberg University, Heidelberg, Germany.
*These authors contributed equally to this work.
†Corresponding author. Email: murthyp@phys.ethz.ch (P.A.M.); defenu@thphys.uni-heidelberg.de (N.D.) ‡Present address: Institute for Quantum Electronics, ETH Zurich, Zurich, Switzerland.

To measure the pair momentum distribution $n(k)$, we used a matter wave focusing technique that has been previously demonstrated for 2D gases (*30*, *31*). First, we rapidly ramped the offset magnetic field to the weakly interacting limit of strongly bound dimers. Immediately after the ramp, we switched off the trapping potential and released the sample to ballistically expand in a shallow harmonic potential for a quarter period $T_{exp}/4 = \pi/2\omega_{exp} = 21.8$ ms, where ω_{exp} is the shallow trap frequency. The $T_{exp}/4$ evolution maps the initial momentum distribution of particles to the spatial distribution. As the time scale of the magnetic field ramp ($\tau_{ramp} \sim 50$ μs) is shorter than the intrinsic time scales of the many-body system, the measured spatial distribution at $t = T_{exp}/4$ reflects, to a very good approximation, the initial momentum distribution of pairs. The strong enhancement of the low-momentum modes in $n(k)$, as seen in Fig. 1D, signals superfluidity in the system as it is related to long-range spatial coherence in the system (*7*, *14*).

In Fig. 1E, we show an example of the measured time-evolution of the in situ $\rho(r,t)$ (orange) and momentum distributions $n(k,t)$ (blue) taken at the interaction parameter $\ln(k_F a_{2D}) \approx 1$. The in situ distribution exhibits periodic compression and expansion at approximately twice the trap frequency ($\omega_B \approx 2\omega_r$), as expected. In contrast, $n(k,t)$ undergoes sharp revivals at twice the rate of $\rho(r)$, i.e., when the cloud size is maximum (outer turning point, $t = t_o$) as well as minimum (inner turning point, $t = t_i$). At intermediate time scales between the turning points, $n(k)$ is broadened. At a qualitative level, this peculiar effect can be understood as a consequence of the oscillation of the hydrodynamic velocity field at any point (x, y), $\mathbf{v_B} \propto \sin(\omega_B t)[x\hat{\mathbf{e}}_\mathbf{x} + y\hat{\mathbf{e}}_\mathbf{y}]$. During the breathing cycle, $\mathbf{v_B}$ vanishes at the two turning points. At the intermediate points, the nonzero value of $\mathbf{v_B}$ manifests in a broadened momentum distribution, whereas the in situ profile shows a monotonous variation between the inner and outer turning points. We provide a more detailed description of the effect using variational Gross-Pitaevskii computations in (fig. S1) (*32*). A similar effect has recently been predicted for the 1D Bose gas in the Tonks-Girardeau regime using scale-invariant dynamics (*33*) and has also been experimentally observed in the weakly interacting regime (*34*).

From these dynamical measurements, the occurrence and violation of scale invariance can be studied by comparing the in situ and momentum-space distributions at different points in time. To illustrate this point, let us consider the time evolution of a scale-invariant gas in a harmonic potential. Naturally, the presence of a trapping potential introduces a length scale and thus explicitly breaks scale invariance. However, as pointed out in (*3*), the special case of a 2D harmonic potential has an inherent SO(2,1) symmetry that restores scaling behavior. Consequently, the harmonically trapped scale-invariant gas displays predictable dynamics with the time-dependent many-body wave function being given in terms of the equilibrium wave function according to

$$\psi(X,t) = \frac{1}{\lambda^N}\psi(X/\lambda, t=0)\times \exp\left(i\frac{m\dot{\lambda}}{2\hbar\lambda}X^2\right)\exp\left(i\theta(t)\right) \quad (1)$$

where $X = (\vec{x}_1, \vec{x}_2, ..., \vec{x}_N)$ are the $2N$ position coordinates of the many-body system, m is the particle mass, $\theta(t)$ is an overall phase, and $\lambda(t)$ is the time-dependent scale factor that obeys the Ermakov-Milne equation (*32*). From the full wave function (Eq. 1), one obtains the evolution of the in situ density and the momentum distribution

$$\rho(\mathbf{r},t) = \frac{1}{\lambda^2}\rho\left(\frac{\mathbf{r}}{\lambda}, t=0\right) \quad (2)$$

$$n(\mathbf{k},t) = \lambda^2\int W\left(\lambda\mathbf{k} + \frac{m}{\hbar}\dot{\lambda}\lambda\mathbf{r}, \mathbf{r}, t=0\right)\mathrm{d}^2\mathrm{r} \quad (3)$$

in terms of the Wigner function $W(\mathbf{k},\mathbf{r},t)$. The in situ density is completely self-similar (Eq. 2), i.e., the density at any time t can be rescaled to its initial form using a single scaling factor $\lambda(t)$. When $\dot{\lambda} = 0$, the momentum distribution $n(k,t)$ also displays self-similar scaling with the inverse factor λ^{-1}. For the breathing modes, $\dot{\lambda} = 0$ at the two turning points. Therefore, a comparison of the in situ and momentum distributions at the inner and outer turning points can be used as a proxy to study scale invariance.

We measured the dynamically evolving in situ and momentum distributions for various interaction parameters across the BEC-BCS crossover. In Fig. 2, we show $\rho(r)$ (left column) and $n(k)$ (right column) at the inner and outer turning points for interaction strengths $\ln(k_F a_{KD}) = -1.5$, 1, 1.3, 1.5, and 2, which correspond to the strongly interacting crossover region. The open diamonds and filled circles represent the distributions at successive inner ($t_{i,1}$, $t_{i,2}$) and outer ($t_{o,1}$, $t_{o,2}$) turning points within a breathing cycle (Fig. 1E). The scaling to the inner turning point distribution is performed using the mean of the successive outer turning point distributions. In the in situ distributions, the outer turning point profile $\rho(r,t_o)$ (blue) can be collapsed onto the inner turning point profile $\rho(r,t_i)$ using a global scaling factor $0 < \lambda < 1$. The rescaling is represented by the dashed black curves in Fig. 2, where $\rho_{sc}(r) = \lambda^{-2}\rho(r/\lambda,t_o)$; the scaling factor λ is obtained by minimizing the mean square deviation between the inner profile and the rescaled outer profile. The measured and rescaled distributions coincide within the systematic and statistical uncertainties of the measured density, which is ~5% (*14*).

In momentum space, the inverse scaling factor λ^{-1} should collapse the inner and outer turning-point distributions if the system were scaling invariant. This condition is satisfied to a good approximation both in the BEC $[\ln(k_F a_{2D}) \lesssim -1.5]$ and BCS $[\ln(k_F a_{2D}) \gtrsim 2]$ regimes (Fig. 2, A and E). In these regimes, the difference between the scaling factor obtained independently for the k-space distributions and the inverse in situ scaling factor is <2%. However, in the crossover region around $\ln(k_F a_{2D}) \sim 1.3$, we find a notable discrepancy between the measured $n(k,t_i)$ at the inner turning point and the rescaled distribution $n_{sc}(k)$ obtained using the inverse in situ scaling factor. In fact, we expect $n(k,t_i)$ to always be broader

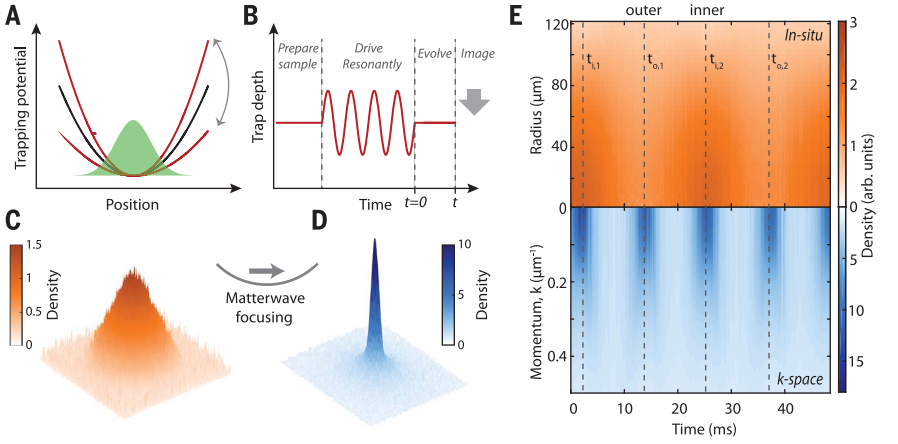

Fig. 1. Dynamics of a 2D fermionic superfluid in position and momentum space. (**A** and **B**) We prepare a 2D Fermi gas well below the superfluid critical temperature ($0.05 < T/T_F < 0.1$) (*14*). The isotropic breathing mode is excited by resonantly modulating the harmonic trap at twice the trap frequency. Once the drive is stopped, the breathing oscillations continue for a variable time t, at which point we measure (**C**) the in situ density distribution $\rho(r,t)$ and (**D**) the pair momentum distribution $n(k,t)$ using a matter wave focusing technique. (**E**) Example of azimuthally averaged $\rho(r,t)$ (orange) and $n(k,t)$ (blue) taken at interaction strength $\ln(k_F a_{2D}) \approx 1$. The in situ density oscillates at twice the trap frequency, as expected. The momentum distribution exhibits sharp revivals at twice the rate of the in situ oscillation. The frequency doubling arises from the sinusoidal oscillation of the hydrodynamic velocity field, which vanishes at the inner and outer turning points of the breathing cycle, denoted by the vertical dashed lines.

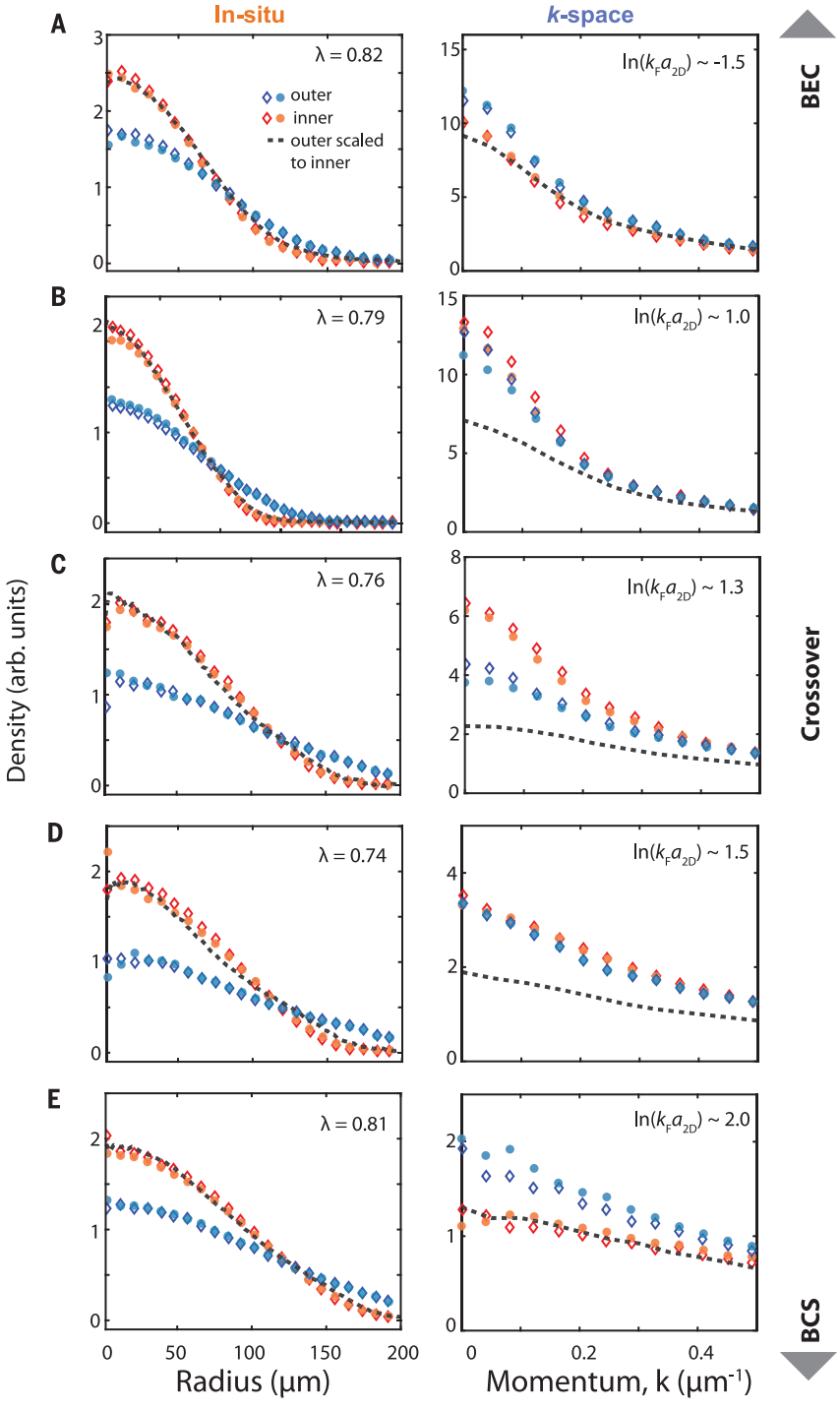

Fig. 2. Scale-invariance breaking in momentum space. The in situ (left column) and pair momentum distributions (right column) at the inner and outer turning points for interaction strengths $\ln(k_F a_{2D}) \approx -1.5$, 1.0, 1.3, 1.5, and 2.0 (**A** to **E**, respectively). The diamonds and filled circles represent the distributions at adjacent inner and outer turning points. For a scale-invariant system, the in situ density profiles at t_o (red diamonds) and t_i (blue circles) should be scalable with a single scaling factor λ, as well as the momentum distributions $[n(k,t_o) \rightarrow n(k,t_i)]$ with the inverse factor λ^{-1}. Such scaling behavior is observed both in the weakly interacting BEC and BCS regimes. However, in the strongly interacting crossover regime, we find a clear departure from scale invariance. Although the evolution of the $\rho(r)$ is still self-similar, the momentum distribution shows a notable discrepancy from the expected result obtained with the inverse scaling factor from the in situ scaling (dashed black line). This scaling violation at strong interactions is attributed to the quantum anomaly.

than $n(k,t_o)$ (see Fig. 2A), but the measured momentum distribution at $\ln(k_F a_{2D}) \sim 1.3$ shows the opposite effect. Here, the occupation of the low-k region of $n(k)$ is strongly enhanced, not only with respect to the expected distribution but also compared with $n(k,t_o)$. This discrepancy is evidence that scale invariance is violated owing to strong interactions, with an unmistakable signature in momentum space.

As shown in Fig. 2, the fermionic interactions have a substantial influence on the low-k modes, which correspond to long-wavelength phase fluctuations in the superfluid. The correlations in the phase are characterized by the first-order correlation function

$$g_1(r) = \int \rho_1(\mathbf{R} - \mathbf{r}/2, \mathbf{R} + \mathbf{r}/2)\, d^2R \qquad (4)$$

where ρ_1 is the one-body density matrix. Experimentally, $g_1(r)$ is directly obtained from the $n(k)$ through a Fourier transform. In (*7*), a transition from exponential to algebraic decay in the trap-averaged $g_1(r)$ was observed, in agreement with BKT theory and quantum Monte Carlo computations (*35*). Here, we use the same procedure described in (*7*) to extract $g_1(r)$ at the inner and outer turning points. These are shown in Fig. 3A for $\ln(k_F a_{2D}) = -6$ and 1.3. To account for the change in cloud size when comparing the two correlation functions, we plot $g_1(\lambda r,t_o)$ in rescaled coordinates, where λ is the scaling factor obtained from the procedure described above (Fig. 2 and Eq. 2). In addition, we extract the exponent η by fitting a power law $[f(r) \sim r^{-\eta(t)}]$ to $g_1(r,t)$. Although the exponents in the trap-averaged $g_1(r)$ are substantially larger than the homogeneous BKT predictions, they have the same qualitative behavior (*35*), in particular, a smaller exponent corresponds to a larger superfluid phase space density $D_s = \rho_s \lambda_T^2$, where ρ_s is the superfluid density and λ_T is the thermal de Broglie wavelength. The power-law exponents obtained at the two turning points are tabulated in table S1 (*32*).

In the BEC regime, the two curves $[g_1(r,t_i)$ and $g_1(\lambda r,t_o)]$ collapse onto each other (Fig. 3A), whereas in the crossover regime, the correlation functions are substantially different, with the inner $g_1(r,t_i)$ decaying slower than expected. In Fig. 3B, we show the ratio η_i/η_o for different interaction strengths across the BEC-BCS crossover. For scale-invariant systems, $\eta_i = \eta_o$, i.e., the spectrum of phase fluctuations is unaffected by a change in the density. Indeed, we find $\eta_i/\eta_o \approx 1$ in the BEC regime, but the ratio dips dramatically in the crossover regime to a value of ~0.8 before rising again in the weakly interacting BCS regime. This quantitative deviation proves that the quantum scale anomaly that originates in the short-distance fermionic correlations influences the algebraic decay of correlations in the 2D superfluid. An equivalent signature is obtained by comparing the outer zero-momentum occupation with the rescaled one at the inner turning point; the resulting curve, shown in the inset of Fig. 3B, also deviates from the scale-invariant expectation in the crossover region.

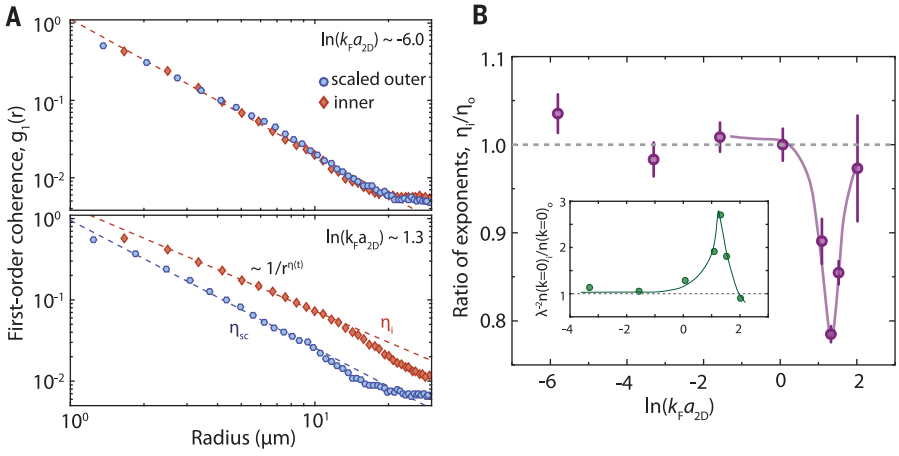

Fig. 3. The quantum anomaly and spatial coherence. (**A**) The first-order correlation function $g_1(r,t_i)$ at inner point (red) and rescaled correlation function $g_1(\lambda r,t_o)$ at the outer points (blue), for $\ln(k_F a_{2D}) \sim -6$ (upper panel, BEC) and $\ln(k_F a_{2D}) \sim 1.3$ (lower panel, crossover), where λ is the real space scaling factor obtained in Fig. 2 . In the BEC regime, $g_1(r,t_i)$ and $g_1(\lambda r,t_o)$ coincide, whereas in the crossover regime, the two curves are conspicuously different. From the power-law decay of $g_1(r) \sim r^{-\eta}$, we extract the exponent η. (**B**) The ratio η_i/η_o across the BEC-BCS crossover. The scale-invariant expectation $\eta_i/\eta_o = 1$ is reproduced in the BEC regime. In the crossover regime, we observe a sharp dip in the ratio signaling the scaling violation in the long-range phase correlations. The minimum ratio is at $\ln(k_F a_{2D}) \sim 1.3$, which coincides with the regime of many-body pairing observed in (*29*). (Inset) The ratio between the zero pair momentum occupation at the inner and outer turning points, divided by $1/\lambda^2$; as above, the largest anomaly is observed in the crossover region. The purple and green curves are guides to the eye.

What is the origin of these effects? The interaction region [$\ln(k_F a_{2D}) \sim 1$] where we see the largest scaling violation in the phase correlations coincides with the regions of (i) maximum critical temperature (*14*), (ii) largest density-dependent pairing (pseudogap) (*29*), and (iii) the maximum breathing mode frequency shift (*26*, *27*). This suggests that all these effects may have a common mechanism. However, the exact dependence of these effects on $\ln(k_F a_{2D})$ is slightly different because local properties such as fermion pairing and long-range properties such as coherence respond differently to temperature. Also, because the breathing motion in the system is much slower than the microscopic scattering rate between fermions, one can apply the traditional hydrodynamic picture where the gas can be considered locally in equilibrium at all times. This allows the dynamical behavior of the gas to be connected with its equilibrium properties.

In this framework, one possible mechanism arises from the density-dependent pairing effect observed in (*29*). In the crossover region, a change in density during the breathing cycle corresponds to a change in the total pairing energy. However, in 2D BCS theory, the coherence length remains fixed to the vacuum expectation a_{2D} irrespective of the density. Accordingly, as the particle spacing is the smallest at the inner turning point, this implies enhanced phase coherence extending over more particle spacings and a smaller decay exponent η. At the same time, enhanced occupation of low-momentum modes requires, at a fixed total number, a reduced occupation at high momenta and hence a depletion in the pair kinetic energy. We have analyzed the kinetic energy extracted from the momentum distribution and found a scaling violation consistent with this argument (fig. S2) (*32*).

The observations in Fig. 3 may also provide hints toward explaining the enhanced critical temperatures in this region. We recall that the power-law exponents are an indicator of superfluid stiffness and phase-space density: a smaller η corresponds to more coherence and greater stiffness D_s. For scale-invariant systems, D_s necessarily remains constant throughout the breathing cycle leading to $\eta_i/\eta_o = 1$. However, in the crossover regime, the observation of $\eta_i/\eta_o < 1$ implies that the density-dependent pair correlations enhance the superfluid phase space density for the same effective temperature. In other words, the critical D_s required for the superfluid transition can be attained at higher T_c/T_F, as seen in (*14*).

Finally, we note the differences between the manifestations of the anomaly in the breathing mode frequency shifts and coherence measurements. The density profiles at the turning points do not exhibit conspicuous effects of the quantum anomaly and satisfy the prediction of the dynamical SO(2,1) symmetry (*24*). This is consistent with the small shifts in the breathing mode frequency reported in (*26*, *27*). It further shows that the breathing mode dynamics are not fully explained by the equation of state (*15*–*17*), which is scale dependent and would imply a large shift in the breathing frequency accompanied by an observable change in the in situ density profile. On the other hand, the coherence of the system probes the long-wavelength phase fluctuations and thus displays a much larger effect of the quantum anomaly. In addition, the coherence properties in the superfluid phase are more sensitive to temperature, which leads to a slightly different dependence on the $\ln(k_F a_{2D})$ with respect to local measurement of many-body pairing (*29*). An important goal for future investigations is to find a theoretical description that connects these different effects—many-body pairing, enhanced critical temperature, breathing mode frequencies, and spatial coherence—in the crossover region. Although the relation between many-body pairing and breathing mode properties has been recently demonstrated theoretically (*36*), the connection between the quantum anomaly and coherence remains an open question.

REFERENCES AND NOTES

1. S. Weinberg, *The Quantum Theory of Fields*, vol. 2 (Cambridge Univ. Press, 1995).
2. B. R. Holstein, *Am. J. Phys.* **61**, 142–147 (1993).
3. L. P. Pitaevskii, A. Rosch, *Phys. Rev. A* **55**, R853–R856 (1997).
4. M. Olshanii, H. Perrin, V. Lorent, *Phys. Rev. Lett.* **105**, 095302 (2010).
5. D. S. Petrov, M. Holzmann, G. V. Shlyapnikov, *Phys. Rev. Lett.* **84**, 2551–2555 (2000).
6. D. S. Petrov, G. V. Shlyapnikov, *Phys. Rev. A* **64**, 012706 (2001).
7. P. A. Murthy *et al.*, *Phys. Rev. Lett.* **115**, 010401 (2015).
8. Z. Hadzibabic, P. Krüger, M. Cheneau, B. Battelier, J. Dalibard, *Nature* **441**, 1118–1121 (2006).
9. R. Balili, V. Hartwell, D. Snoke, L. Pfeiffer, K. West, *Science* **316**, 1007–1010 (2007).
10. O. Ovdat, J. Mao, Y. Jiang, E. Y. Andrei, E. Akkermans, *Nat. Commun.* **8**, 507 (2017).
11. Y. Cao *et al.*, *Nature* **556**, 43–50 (2018).
12. C.-L. Hung, X. Zhang, N. Gemelke, C. Chin, *Nature* **470**, 236–239 (2011).
13. R. Desbuquois *et al.*, *Phys. Rev. Lett.* **113**, 020404 (2014).
14. M. G. Ries *et al.*, *Phys. Rev. Lett.* **114**, 230401 (2015).
15. V. Makhalov, K. Martiyanov, A. Turlapov, *Phys. Rev. Lett.* **112**, 045301 (2014).
16. I. Boettcher *et al.*, *Phys. Rev. Lett.* **116**, 045303 (2016).
17. K. Fenech *et al.*, *Phys. Rev. Lett.* **116**, 045302 (2016).
18. G. Bertaina, S. Giorgini, *Phys. Rev. Lett.* **106**, 110403 (2011).
19. H. Shi, S. Chiesa, S. Zhang, *Phys. Rev. A* **92**, 033603 (2015).
20. J. Hofmann, *Phys. Rev. Lett.* **108**, 185303 (2012).
21. S. Moroz, *Phys. Rev. A* **86**, 011601 (2012).
22. C. Gao, Z. Yu, *Phys. Rev. A* **86**, 043609 (2012).
23. W. Daza, J. E. Drut, C. Lin, C. Ordóñez, *Phys. Rev. A* **97**, 033630 (2018).
24. E. Taylor, M. Randeria, *Phys. Rev. Lett.* **109**, 135301 (2012).
25. E. Vogt *et al.*, *Phys. Rev. Lett.* **108**, 070404 (2012).
26. M. Holten *et al.*, *Phys. Rev. Lett.* **121**, 120401 (2018).
27. T. Peppler *et al.*, *Phys. Rev. Lett.* **121**, 120402 (2018).
28. P. Dyke *et al.*, *Phys. Rev. A* **93**, 011603 (2016).
29. P. A. Murthy *et al.*, *Science* **359**, 452–455 (2018).
30. S. Tung, G. Lamporesi, D. Lobser, L. Xia, E. A. Cornell, *Phys. Rev. Lett.* **105**, 230408 (2010).
31. P. A. Murthy *et al.*, *Phys. Rev. A* **90**, 043611 (2014).
32. See supplementary materials.
33. Y. Y. Atas, I. Bouchoule, D. M. Gangardt, K. V. Kheruntsyan, *Phys. Rev. A* **96**, 041605 (2017).
34. B. Fang, G. Carleo, A. Johnson, I. Bouchoule, *Phys. Rev. Lett.* **113**, 035301 (2014).
35. I. Boettcher, M. Holzmann, *Phys. Rev. A* **94**, 011602 (2016).
36. T. Enss, Dynamical viscosity, contact correlations and pairing in attractive Fermi gases. arXiv:1904.12772 [cond-mat. quant-gas] (29 April 2019).

37. P. A. Murthy, N. Defenu, L. Bayha, M. Holten, P. M. Preiss, T. Enss, S. Jochim, Quantum anomaly and spatial coherence in a 2D Fermi superfluid, Version 1, Zenodo (2019); https://doi.org/10.5281/zenodo.2624085V.

ACKNOWLEDGMENTS

We thank I. Boettcher, T. Gasenzer, J. Hofmann, K. V. Kheruntsyan, T. Lompe, and S. Moroz for insightful discussions. **Funding:** This work has been supported by the ERC consolidator grant 725636, the Heidelberg Center for Quantum Dynamics, and is part of the DFG Collaborative Research Center SFB 1225 (ISOQUANT). P.M.P. acknowledges funding from the European Union's Horizon 2020 program under Marie Skłodowska-Curie grant agreement 706487. **Author contributions:** P.A.M. performed the measurements and data analysis. N.D. and T.E. provided the theoretical description of the observations. L.B., M.H., and P.M.P. assisted with experiments and interpretation of data. T.E. and S.J. supervised the project. P.A.M. and N.D. conceptualized and wrote the manuscript. **Competing interests:** The authors declare no competing interests. **Data and materials availability:** Data shown in this paper are deposited in (*37*).

SUPPLEMENTARY MATERIALS

science.sciencemag.org/content/365/6450/268/suppl/DC1
Materials and Methods
Supplementary Text
Figs. S1 to S3
Table S1
References (*38*, *39*)

11 June 2018; accepted 18 June 2019
10.1126/science.aau4402

Quantum scale anomaly and spatial coherence in a 2D Fermi superfluid

Puneet A. Murthy, Nicolò Defenu, Luca Bayha, Marvin Holten, Philipp M. Preiss, Tilman Enss and Selim Jochim

Science **365** (6450), 268-272.
DOI: 10.1126/science.aau4402

A quantum breakdown

At low temperatures, two-dimensional (2D) systems with contact interactions are expected to exhibit quantum anomalies—a breakdown of scaling laws that characterize such systems in the classical regime. Signatures of these anomalies have been observed in the real-space properties of 2D Fermi gases, but the effect is much less pronounced than expected on theoretical grounds. Murthy *et al.* studied the momentum-space profiles of 2D superfluids of fermionic atoms. They initially perturbed the gas and then monitored the momentum distribution of its atoms. In the regime of strong interactions between the atoms, the momentum profiles deviated markedly from the classical scaling.

Science, this issue p. 268